Journal of the European Ceramic Society **12** (1993) 287–296

Densification, Microstructure and Properties of Si_3N_4–Ti(C,N) Composites

M. Herrmann, B. Balzer, Chr. Schubert & W. Hermel

Fraunhofer-Einrichtung für Keramische Technologien und Sinterwerkstoffe (IKTS), Winterbergstr. 28, O-8020 Dresden, Germany

(Received 26 March 1993; revised version received 4 June 1993; accepted 18 June 1993)

Abstract

Dense Si_3N_4–TiN composites with 20–50 wt% TiN with various grain sizes were produced by hot pressing and gas-pressure sintering under nitrogen gas atmosphere. The dependence of the densification behaviour on the TiN content and on the grain size of TiN was investigated. Starting from the thermodynamical considerations the influence of the C-content in the Ti(C,N) on the densification was analysed and tested by experiment.

Dichte Si_3N_4–TiN-Kompositwerkstoffe mit 20–50 wt% TiN unterschiedlicher Korngröße wurden mittels Heißpressen und Gasdrucksintern hergestellt. Dabei wurde die Abhängigkeit des Verdichtungsverhaltens vom TiN-Gehalt und der TiN-Korngröße untersucht. Ausgehend von thermodynamischen Überlegungen wurde der Einfluß des C-Gehaltes im Ti(C,N) auf die Verdichtung analysiert und experimentell überprüft.

Des composites denses de Si_3N_4–TiN avec 20–50 wt% de TiN, de tailles de grains différentes, ont été fabriqués par pressage à chaud et frittage sous pression d'azote. L'influence du contenu en TiN et de la taille des grains de TiN sur la densification a été étudiée. On a analysé l'influence du contenu en carbone dans la phase Ti(C,N) sur la densification à partir de considérations thermodynamiques, et testé cette analyse expérimentalement.

1 Introduction

Silicon nitride is one of the most promising candidates among technical ceramics. A broad use of these materials has up to now been limited by the relatively low fracture toughness and reliability as compared with metals.

Recently the development of high-strength and high-toughness ceramics by whisker or particle reinforcement has started to improve the mechanical properties and the wear behaviour. The production of whisker composites leads to a lot of technological problems. That is why particle reinforcement has received increasing attention. The particle-reinforced composites with nitrides, carbides and borides of the transition elements (TiN, TiC, TiB_2, ZrN) have found some special applications as cutting tools. Their good electrical conductivity also results in their use as heating elements, igniters and heat exchangers. The electrical conductivity has a second advantage. By using electrically discharged machines it is possible to produce components of complex shape.[1–4]

There are a few data about sintering and properties of such materials,[5–9] but a systematic investigation into the sintering behaviour, the microstructure and the properties of such composites does not exist. That is why the goal of this paper is the investigation of sintering as a function of the amount and the grain size of TiN and of the composition of $TiC_{1-x}N_x$.

In a further paper the microstructure and properties will be explained.

2 Experimental Methods

Commercial powders, Si_3N_4 (LC12S, HCST) and TiN (grade B and C, HCST) or Ti(C,N) (HCST), Y_2O_3 (fine grade, HCST) and Al_2O_3 (A16, AlCOA), were used for the investigations. Two series of samples were prepared (Tables 1, 2 and 3):

—The first group of materials contained a constant quantity of the sintering additives (5 wt% Y_2O_3 and 2 wt% Al_2O_3) independent of the amount of TiN or Ti(C,N). This means that the volume fraction of the liquid phase during sintering was nearly constant. TiN (grade C) and

Journal of the European Ceramic Society 0955-2219/93/$6.00

Table 1. Composition of the tested materials of the first group

Sample	Composition					Density		Sintering temperature
	Si_3N_4 (wt%)	Y_2O_3 (wt%)	Al_2O_3 (wt%)	TiCN (wt%)	C/(C+N) (%)	(g/cm³)	(%)	(°C)
Gas-pressure sintering								
Si_3N_4	93	5	2	—	—	3·18	98·7	1 800
						3·23	100	1 850
						3·24	100	1 900
C/N-0/1	63	5	2	30	30	3·55	99·2	1 800
						3·66	100	1 850
						3·68	100	1 900
C/N-3/7	63	5	2	30	30	3·55	97·2	1 800
						3·66	100	1 850
						3·68	100	1 900
C/N-5/5	63	5	2	30	50	3·35	92·3	1 800
						3·45	94·8	1 850
						3·68	96·5	1 900
C/N-1/0	63	5	2	30	100	3·35	85·0	1 800
						3·45	79·3	1 850
						3·68	70·2	1 900
Hot-pressing								
Si_3N_4	93	5	2	—	—	3·23	100	—
T20/C	73	5	2	20	0	3·52	100	—
T30/C	63	5	2	30	0	3·68	100	—
T40/C	53	5	2	40	—	3·87	100	—
TCN3/7	63	5	2	30	30	3·68	100	—
TCN7/3	63	5	2	30	70	3·67	100	—

Table 2. Composition of the gas-pressure sintered materials of the second group

Sample	Composition					Density		Sintering temperature
	Si_3N_4 (wt%)	Y_2O_3 (wt%)	Al_2O_3 (wt%)	TiN (wt%)	Fraction	(g/cm³)	(%)	(°C)
T40/1	55·8	3	1·2	40	1	3·53	91·6	1 800
						3·78	98·1	1 850
						3·74	97·1	1 900
T40/2	55·8	3	1·2	40	2	3·47	90·2	1 800
						3·66	95·1	1 850
						3·70	96·2	1 900
T20/3	74·4	4	1·6	20	3	3·32	94·6	1 800
						3·38	96·4	1 850
						3·45	98·4	1 900
T30/3	65·1	3·5	1·4	30	3	3·38	92·1	1 800
						3·49	95·1	1 850
						3·61	98·4	1 900
T40/3	55·8	3	1·2	40	3	3 38	87·9	1 800
						3·52	91·5	1 850
						3·63	94·4	1 900

Ti(C,N)-30/70 or Ti(C,N)-50/50 were used as dispersoids.

—The second group was prepared with a constant ratio of Si_3N_4/sintering additives (5 wt% Y_2O_3 + 2 wt% Al_2O_3:93 wt% Si_3N_4). The amount and the grain size of TiN was varied. For these materials the TiN powder (grade B) was separated into three fractions by jet milling (AFG-50) under nitrogen. The resulting particle size distributions of the three fractions are given in Fig. 1.

The first group of materials was produced by mixing the materials in an isopropanolic solution in a laboratory attrition mill. The vessel of the mill was made of Al_2O_3, the balls and the stirring arm of Si_3N_4. To achieve a good homogenization and distribution of the big agglomerates of TiN, the material was intensively milled at 1000 rpm for 4 h. The materials containing Ti(C,N) were also homogenized under such conditions.

The materials of the second group were prepared in a two-step process. At the first step the Si_3N_4 and

Table 3. Composition and properties of the hot-pressed materials of the second group (the confidence interval of strength is given; $p > 95\%$)

Sample	*Composition*					*Density* (g/cm^3)	*Strength* (*MPa*)
	Si_3N_4 (*wt%*)	Y_2O_3 (*wt%*)	Al_2O_3 (*wt%*)	*TiN* (*wt%*)	*Fraction*		
T20/1	74·4	4	1·6	20	1	3·51	914 ± 51
T30/1	65·1	3·5	1·4	30	1	3·67	918 ± 53
T40/1	55·8	3	1·2	40	1	3·85	815 ± 39
T50/1	46·5	2·5	1	50	1	4·04	863 ± 50
T20/2	74·4	4	1·6	20	2	3·51	643 ± 119
T30/2	65·1	3·5	1·4	30	2	3·68	784 ± 82
T40/2	55·8	3	1·2	40	2	3·85	813 ± 35
T50/2	46·5	2·5	1	50	2	4·04	791 ± 22
T20/3	74·4	4	1·6	20	3	3·51	745 ± 39
T30/3	65·1	3·5	1·4	30	3	3·67	762 ± 15
T40/3	55·8	3	1·2	40	3	3·85	678 ± 48
T50/3	46·5	2·5	1	50	3	4·05	712 ± 25

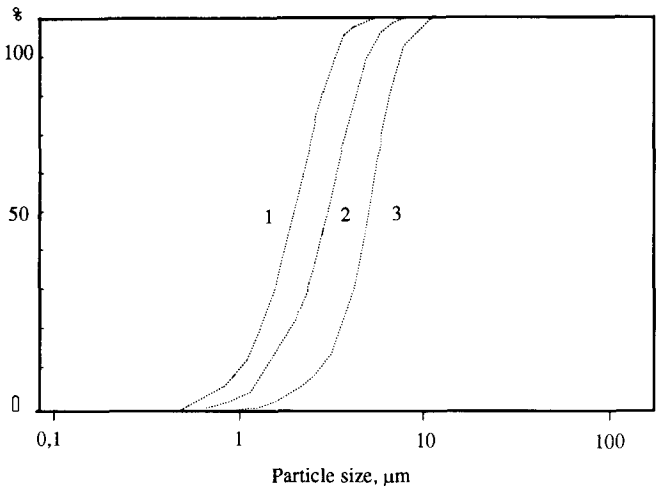

Fig. 1. Particle size distribution of the TiN fractions.

the sintering additives were mixed in the attrition mill and then dried. Mixing with TiN was carried out in the ball mill for 2 h. The vessel of the mill and the balls were made of agate. The pick up of the SiO_2 during the milling process was less than 0·2%.

For gas pressure sintering the bars ($5 \times 5 \times 60\,mm^3$) were pressed at 200 MPa. The achieved green densities were about 58% of the theoretical value.

Before hot pressing and sintering the binder was baked thoroughly at 280°C for 8 h in air for the TiN–Si_3N_4 composites and up to 500°C in argon for the Ti(CN)–Si_3N_4 composites. Such a low temperature was used to prevent oxidation of the TiN. The content of carbon in the TiN samples after baking was 0·1 wt%. The increase of oxygen during thermal treatment of binder-free mixture with 50% of the finest TiN fraction was 0·2%, showing the absence of oxidation of TiN.

The sintering was carried out under nitrogen in a gas-pressure furnace (FPW 150/200, KCE, Germany) with a carbon heater. The densification was measured by a dilatometer in the furnace. The specimens were sintered in a crucible of RBSN, specimens containing Ti(C,N) both in a RBSN crucible and in a powder bed (Si_3N_4; grain size $< 100\,\mu m$) in a BN-coated graphite crucible.

Hot pressing was carried out in a hot press (HPW 200/250-180, KCE, Germany) under nitrogen. The densification was controlled by measuring the displacement of the plunger, which was corrected by the dilatation of the device with a dense Si_3N_4 sample.[10] For the calculation of the densification curves and shrinking rate a special programme, JP-8, developed in our institute,[10] was used.

3 Results and Discussion

3.1 Thermodynamic calculations of the stability of the composites

Values of the thermodynamic equations were taken from the literature.[11]

The calculations show that Si_3N_4–TiN is stable under sintering conditions. Investigations[12,13] into the TiN–Si_3N_4 system show that there is a formation of a limited solid solution of Si_3N_4. The TiO_2 surface layer of the TiN reacts with Si_3N_4 according to the following equations:

$$6TiO_2 + 4Si_3N_4 \rightarrow 6TiN + 12SiO + 5N_2 \quad (1)$$

$$6TiO_2 + 2Si_3N_4 \rightarrow 6TiN + 6SiO_2 + N_2 \quad (2)$$

At 2100 K the equilibrium pressure of the equations is 100 MPa. This means that the TiO_2 reacts nearly completely with SiO_2 and TiN and is not stable under sintering conditions. TiO_2 can take part in the formation of a low viscosity liquid only at the initial stage of sintering.

The interactions in the Si_3N_4–TiC system are more complex, because TiC can form a solid solution with TiN.[12,13] From hard metal production it is known that the reaction

$$[TiC] + \tfrac{1}{2}N_2 \leftrightarrow [TiN] + C(s) \quad (3)$$

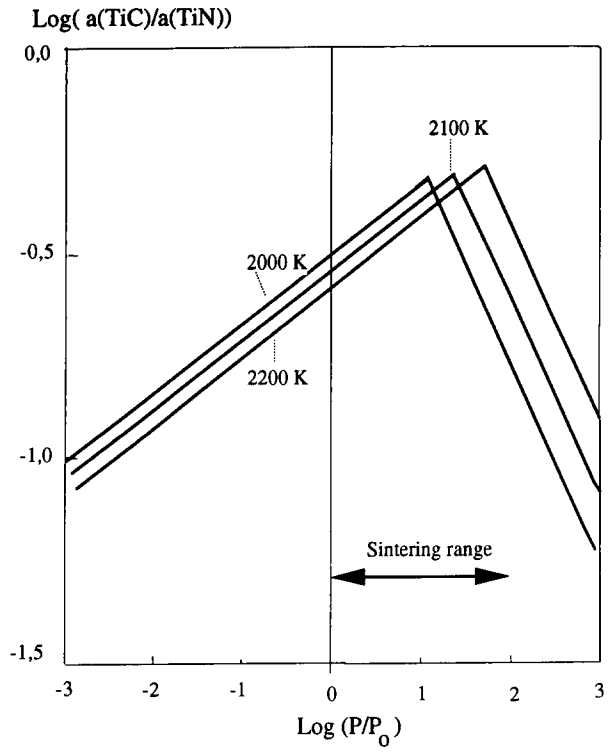

Fig. 2. The dependence of the TiC/TiN activity relation on the equilibrium partial pressure of nitrogen and the temperature ($P_0 = 0{\cdot}1$ MPa).

can take place under sintering conditions ([ ] means that these are components of the solid solution). The resulting solid solution has the form $TiC_{1-x}N_x$.[12,13]

Si_3N_4 reacts with TiC according to the following equation:

$$6[TiC] + 2Si_3N_4 \rightarrow 6[TiN] + 6SiC + N_2 \quad (4)$$

The dependence of the equilibrium ratio of the activities of the solid solution a_{TiN}/a_{TiC} components on the nitrogen pressure is shown in Fig. 2. If the nitrogen pressure is lower than the equilibrium pressure for the reaction

$$Si_3N_4 + 3C \rightarrow 3SiC + 2N_2 \quad (5)$$

eqn (4) determines the equilibrium ratio a_{TiN}/a_{TiC}. With rising nitrogen pressure the stability of Si_3N_4 increases and therefore the content of TiC in the solid solution also increases.

If the nitrogen pressure is higher than the equilibrium pressure of eqn (5), Si_3N_4 is in equilibrium with carbon, and the amount of TiC in the solid solution $TiC_{1-x}N_x$ is determined by its own stability (eqn (3)). The maximum equilibrium ratio a_{TiC}/a_{TiN} is nearly independent of the temperature (Fig. 2) and is about $TiC_{0{\cdot}3}N_{0{\cdot}7}$ (under the assumption that $c_{TiC}/c_{TiN} = a_{TiC}/a_{TiN}$).

In addition to the interaction of TiC with Si_3N_4, the reaction of TiC with the sintering additives and the silicon dioxide must be taken into account:

$$6[TiC] + 2SiO_2 + 3N_2 \rightarrow 6[TiN] + 2SiC + CO \quad (6)$$

$$6[TiC] + 3SiO_2 + 5N_2 \rightarrow 6[TiN] + Si_3N_4 + 6CO \quad (7)$$

$$2Al_2O_3 + 6[TiC] + 5N_2 \rightarrow 4AlN + 6[TiN] + 6CO \quad (8)$$

$$2Al_2O_3 + 9[TiC] + 4{\cdot}5N_2 \rightarrow Al_4C_3 + 9[TiN] + 6CO \quad (9)$$

These reactions depend not only on the nitrogen pressure but also on the CO partial pressure and on the activity of SiO_2 and Al_2O_3 in the liquid phase. Figures 3 and 4 give the dependence of the a_{TiC}/a_{TiN} ratio on these parameters. At high nitrogen pressure something like a carbonitridation of SiO_2 and Al_2O_3 occurs. At low nitrogen pressure SiC and Al_4C_3 are formed.

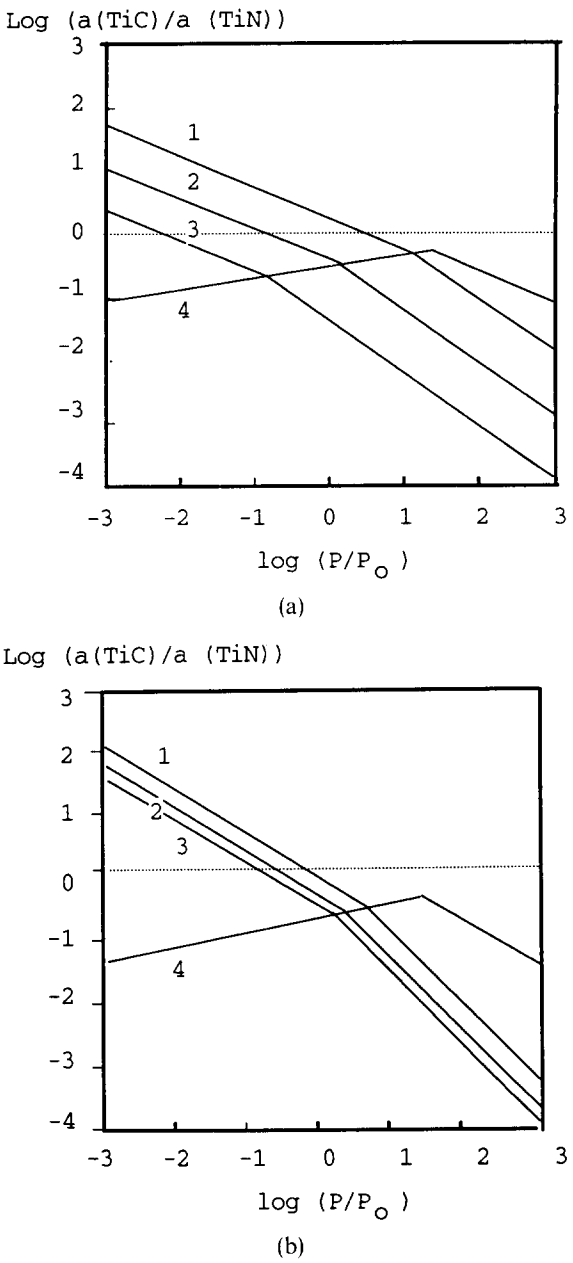

Fig. 3. The dependence of the TiC/TiN activity relation at 2100 K on (a) the CO pressure ($a_{SiO_2} = 1$); 1, $a_{CO} = 1$ MPa; 2, $a_{CO} = 0{\cdot}1$ MPa; 3, $a_{CO} = 0{\cdot}01$ MPa; 4, eqns (3) and (4); (b) the SiO_2 concentration ($P_{CO} = 0{\cdot}1$ MPa); 1, $a_{SiO_2} = 1$ MPa; 2, $a_{SiO_2} = 0{\cdot}5$ MPa; 3, $a_{SiO_2} = 0{\cdot}1$ MPa; 4, eqns (3) and (4); $P_0 = 0{\cdot}1$ MPa.

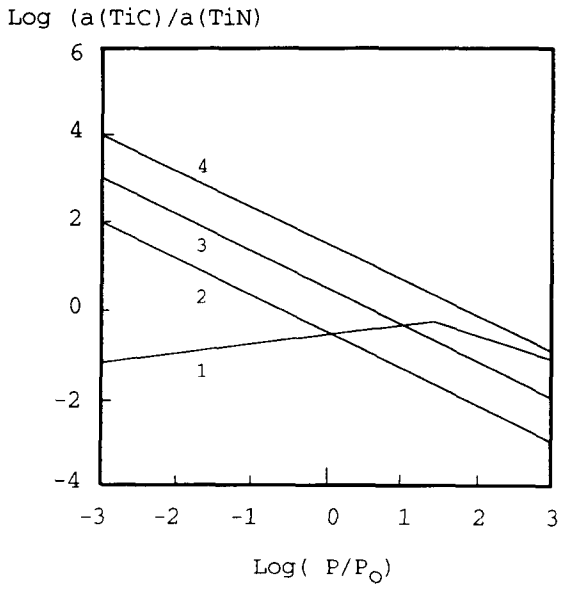

Fig. 4. The dependence of the TiC/TiN activity relation at 2100 K on the CO pressure ($a_{Al_2O_3} = 1$); $P_0 = 0{\cdot}1$ MPa. 1, eqns (3) and (4); 2, $a_{CO} = 0{\cdot}01$ MPa; 3, $a_{CO} = 0{\cdot}1$ MPa; 4, $a_{CO} = 1$ MPa.

Figures 3 and 4 show that the stability of Al_2O_3 is higher than the stability of SiO_2. The same result can be obtained for Y_2O_3. That is why the reduction of the amount of the liquid phase takes place mainly by decomposition of SiO_2. Al_2O_3 and Y_2O_3 can be used more effectively for the densification.

The thermodynamic calculations show that a high CO partial pressure is favourable for the densification of Si_3N_4–TiC composites. But the increase of the CO partial pressure leads to a higher corrosion of the heater and to a reduction in reproducibility due to the transport reactions:

$$CO \rightarrow C + CO_2 \quad \text{(low temperatures)} \quad (10)$$

$$CO_2 + C \rightarrow CO \quad \text{(high temperatures)} \quad (11)$$

These reactions lead to the precipitation of carbon on cold parts of the furnace and increased corrosion of the heater.

3.2 Sintering kinetics of Si_3N_4–TiN composites

The densification behaviour during the hot pressing of the materials of the first and second group of Si_3N_4–TiN materials is shown in Figs 5 and 6. The sintering behaviour of the materials does not change drastically with the variation of the amount of TiN.

There exist two main stages of sintering. At temperatures below 1550°C the main mechanism for the densification is rearrangement and viscous flow. The densification starts at 1300–1400°C before the load is applied. It increases with rising content of TiN in this temperature range (Fig. 5). The main reason for this seems to be the formation of a low-viscosity liquid due to the TiO_2 content. Samples with a higher TiO_2 content (partially oxidized TiN)

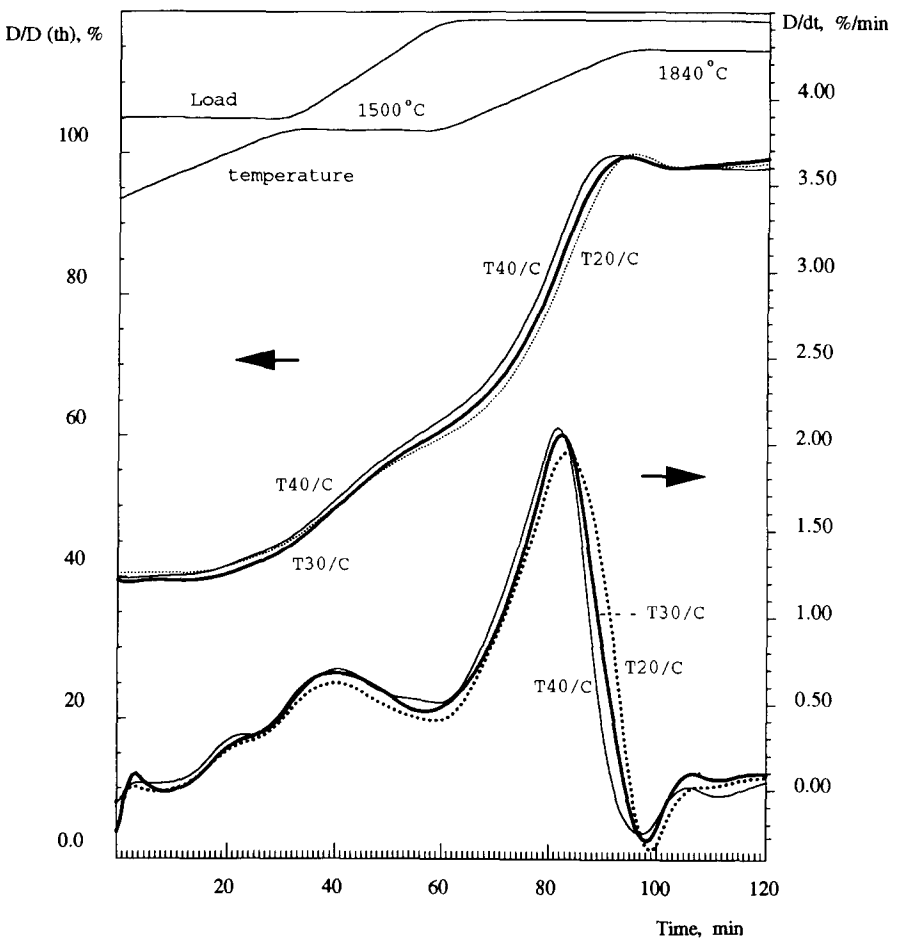

Fig. 5. Densification and densification rate during the hot pressing depending on the amount of TiN.

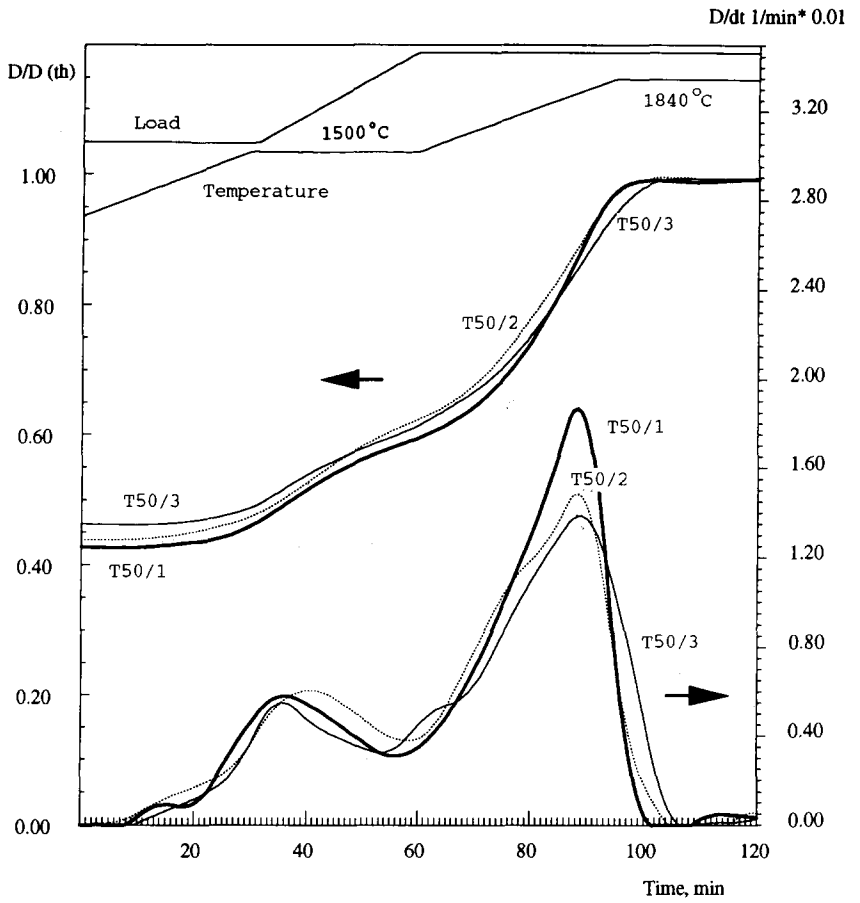

Fig. 6. Densification and densification rate during the hot pressing of materials with 50 wt% TiN and different grain size.

also show a higher densification rate in this temperature range. The increasing load accelerates these processes (Figs 5 and 6). The intensity of the rearrangement and viscous flow rise with increasing TiN content in the first group of materials and do not correlate with the TiN content and grain size in the second group. At the end of the isothermal heating period at 1500 °C the density of the materials of the second group is independent of the composition. The materials with the lower initial density undergo a higher densification during the first sintering stage. The second stage of sintering is caused by solution–diffusion–precipitation accompanied by the viscous flow. It is influenced by the amount of the liquid phase and the amount and grain size of TiN.

If the volume of the liquid phase during hot pressing is nearly independent of the TiN content

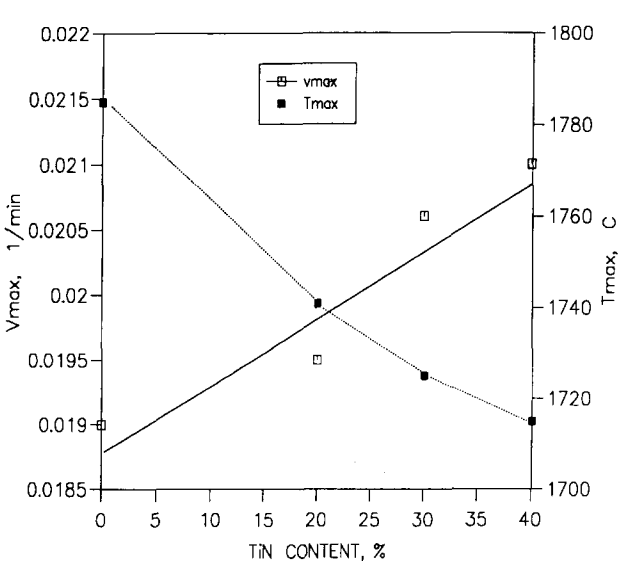

Fig. 7. The dependence of the shrinking rate (v_{max}) and of the temperature (T_{max}) of the maximum densification on the TiN content for the materials of the first group.

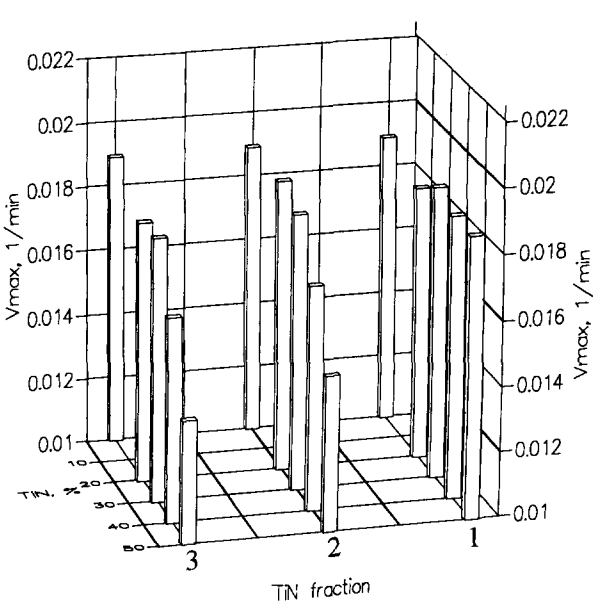

Fig. 8. Maximum shrinking rate (v_{max}) during the hot pressing as a function of the TiN content and TiN grain size.

(first group of materials), the maximum shrinking rate v_{max} increases and the temperature at which v_{max} is reached decreases with increasing TiN content (Fig. 7). In the materials with the decreasing amount of sintering additives (second group) the shrinking rate maximum v_{max} remains constant for the fine fraction of the TiN grains and decreases for the coarser TiN fractions (Fig. 8). The temperature of the maximum shrinking rate for the second group of the materials is independent of the grain size and amount of TiN. This effect cannot be explained by a difference in the oxygen content of the materials with the different TiN fractions, because for the samples with 30% TiN the oxygen content after binder burn out was $3{\cdot}3 \pm 0{\cdot}15\%$. Additionally previous investigations[13] show that the partial oxidation of the TiN or TiC influences the densification mainly in the temperature range 1200–1400°C, e.g. during the rearrangement. Figure 9 shows the dependence of the maximum shrinking rate on the grain size of TiN for the materials with 30 wt% TiN. It is obvious that the fine TiN accelerates the densification and the coarse fraction of TiN slows it down. The investigations into the composition of TiN grains (diameter 5 μm) by microanalysis show no evidence of the incorporation of Si or oxygen in the TiN grains.[12] The formation of the solid solution of Si_3N_4 in TiN under equilibrium conditions[14] seems to be hindered by kinetics. This proves that the TiN grains do not dissolve completely in the oxynitride liquid. However, the microstructures of the materials prepared at different temperatures show a slight grain growth with increasing temperature. Also the shape of the grains changes during the sintering (Fig. 10). These facts prove that TiN contributes in the densification by solution–diffusion–precipitation.

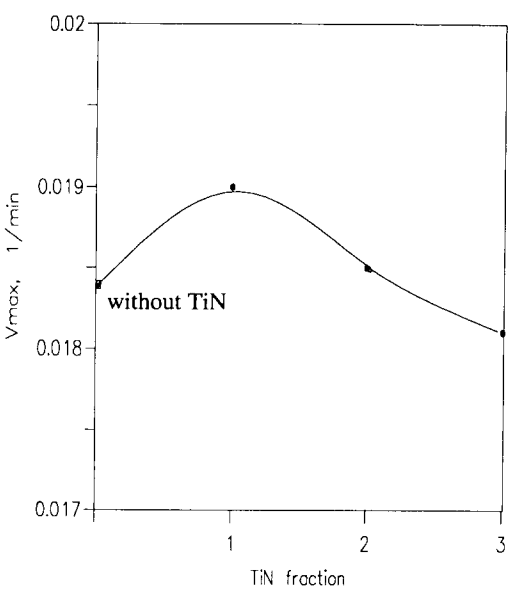

Fig. 9. Dependence of the maximum densification rate during the hot pressing on the grain size of TiN of materials with 30 wt% TiN.

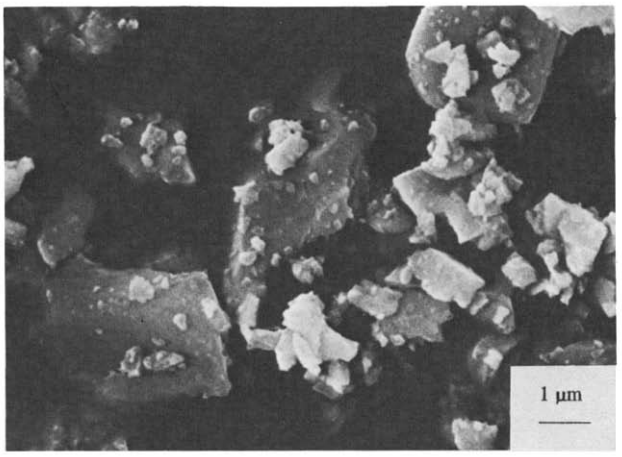

(a)

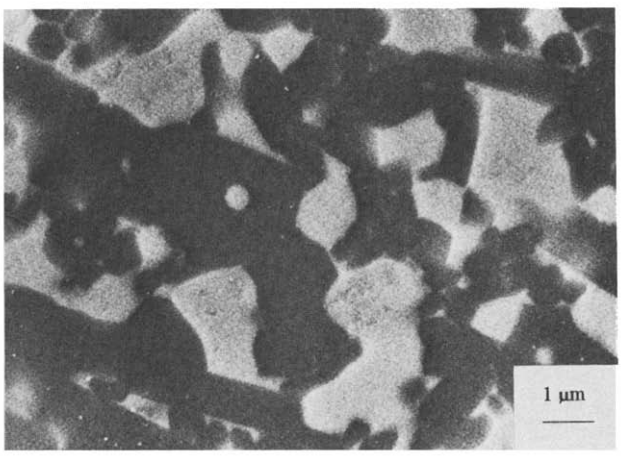

(b)

Fig. 10. SEM micrographs of (a) the TiN powder (grade C) and (b) of a polished section of the hot-pressed material (white area TiN).

Theoretical and experimental investigations into the influence of non-sintering inclusions on the densifications[15,16] show that with rising amount and decreasing grain size of the inclusion the densification deteriorates. The investigations into the system Si_3N_4–TiN give an inverse dependence. This is additional evidence supporting the conclusion that TiN takes part in the sintering process and cannot be considered as a rigid inclusion. The same relations between sinterability and TiN content and grain size were found for the gas-pressure sintering of TiN, as shown in Figs 11 and 12. The main difference to hot pressing is that the hindrance of densification by the coarser TiN fraction is stronger.

3.3 Sintering kinetics of the Si_3N_4–Ti(C,N) composites

As already mentioned, TiCN is not stable under sintering conditions. The densification rate of Si_3N_4–TiCN composites decreases with increasing carbon content of $TiC_xN_{(1-x)}$ (Fig. 13). The interpretation of the densification rate up to 1500°C is not completely clear and depends on small

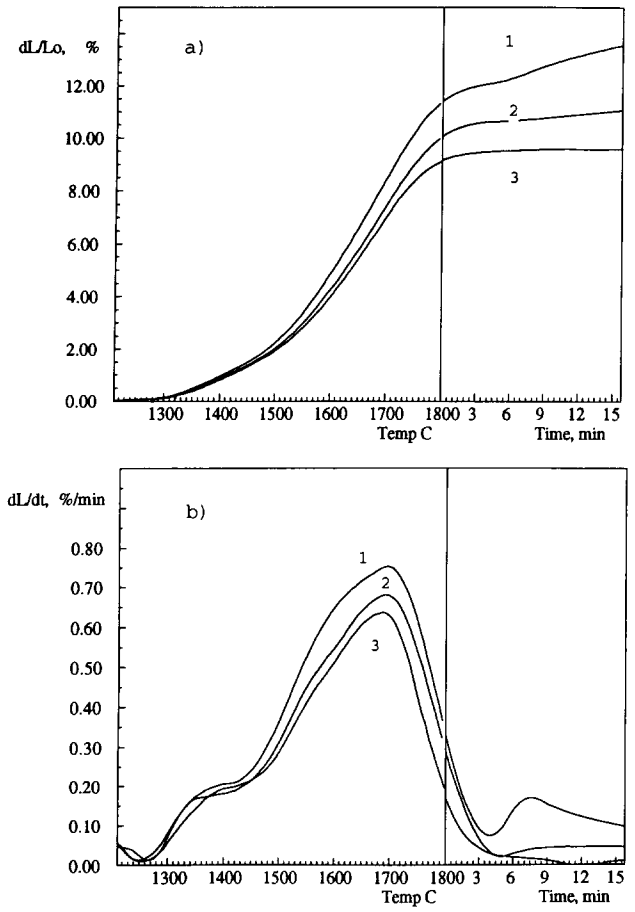

Fig. 11. (a) Shrinking and (b) shrinking rate of the materials with 40% TiN; 1, TiN fraction 1; 2, TiN fraction 2; 3, TiN fraction 3.

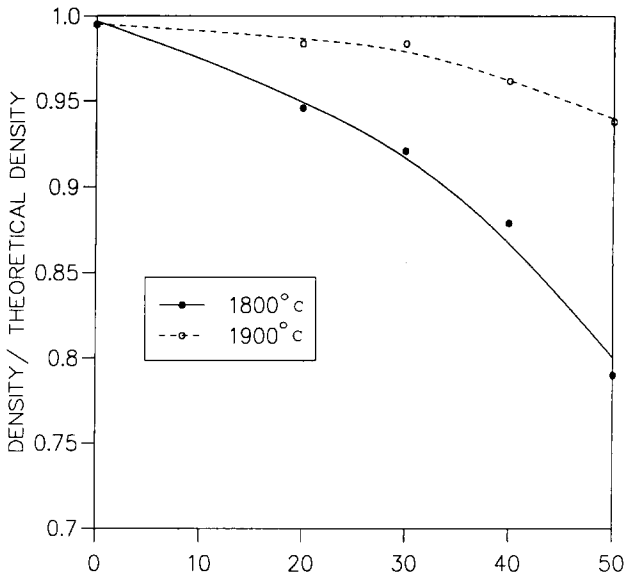

Fig. 12. Dependence of the density after sintering on the amount of TiN (fraction 3).

variations of the initial density, grain size and oxygen content of the TiC and TiCN powders. It decreases with increasing carbon content. This is connected with the reduction of the TiO_2 at the surface of the TiCN according to eqn (1) and with the reduction of the oxynitride liquid phase. These two processes decrease the amount of the liquid during sintering. The rate of these reactions (eqns (6) and (9)) increases with increasing temperature.

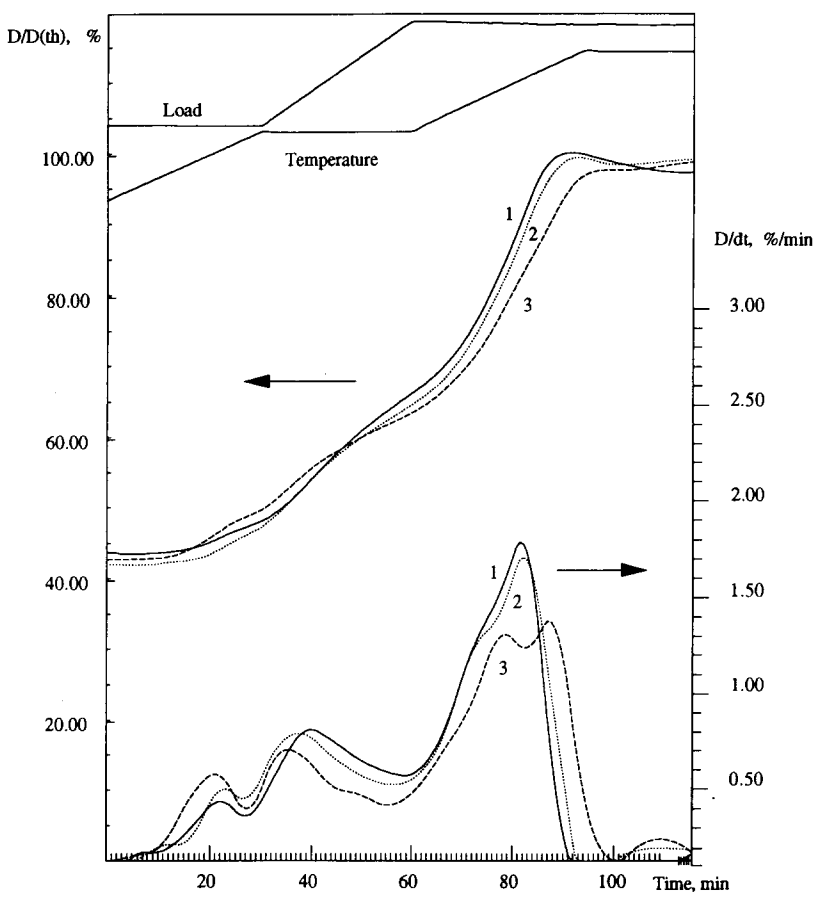

Fig. 13. Densification and densification rate during the hot pressing of materials with 30% Ti(C,N) with different compositions (1, TiN; 2, $TiC_{0.3}N_{0.7}$; 3, $TiC_{0.7}N_{0.3}$).

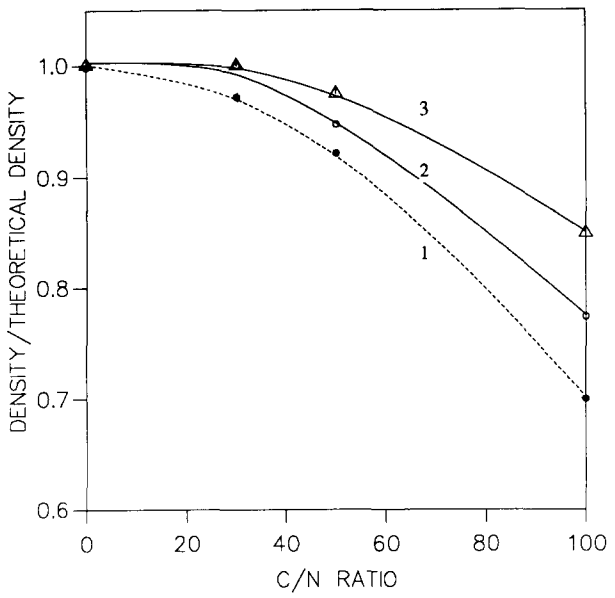

Fig. 14. Dependence of the density after the gas-pressure sintering on the initial C/N ratio in the $TiC_{1-x}N_x$.

Investigations with ESMA show that a gradient of the N and C concentration exists inside the TiC grains after hot pressing.[12] It seems that the nitridation of the TiC is limited by diffusion at this temperature range. That is why a good densification is possible when a fast densification can be achieved, as during hot pressing.

In the case of gas-pressure sintering the densification behaviour depends more intensively on the C content of the $TiC_xN_{(1-x)}$ (Fig. 14). The higher isothermal sintering temperature leads to a faster and more complete densification. At the beginning of the isothermal period at 1850°C or 1900°C the density achieved is 92·5% or 95%, respectively, for the material TiC/N5/5-30. Figure 13 shows that the influence of the C/(N + C) ratio <0·3 on the final density is small. This is in keeping with the thermodynamical calculations (Fig. 4) and the measured carbon content in the compounds after sintering at 1900°C. These EDX measurements show no significant change in the composition of the $TiC_{0·3}N_{0·7}$ and reduction of the carbon content in the materials with $TiC_{0·5}N_{0·5}$ to the composition $TiC_{0·4}N_{0·6}$. At a C/(N + C) ratio higher than 0·3 the density of the sintered sample decreases with increasing carbon content. According to eqns (6)–(9) a higher CO content leads to higher density because the reduction of the liquid phase and the shift of the C/N ratio in the TiCN grains is smaller. So the parameter of the cubic lattice of the $TiC_{0·5}N_{0·5}$ after normal sintering is 0·4266 nm, which corresponds to the $TiC_{0·35}N_{0·65}$ composite. After sintering under a higher CO partial pressure the lattice constant is 0·4275 nm, indicating a higher carbon content in the TiCN.

The mechanical properties of the matrials are given in Tables 3 and 4. The detailed discussion of the relations between the microstructure and properties are given in the second part of this paper.

4 Conclusions

(1) Fine-grained TiN accelerates the densification of Si_3N_4. With increasing grain size the densification is retarded.

(2) The TiO_2 at the surface of the TiCN forms an intermediate liquid at the start of the sintering process. At higher temperatures the TiO_2 is reduced to TiN.

(3) The TiN takes part in the solution–diffusion–precipitation stage.

(4) With increasing carbon content of the $TiC_xN_{(1-x)}$ particles it is more difficult to obtain fully densified materials. This is connected with the instability of $TiC_xN_{(1-x)}$ with $x > 0·3$–$0·4$ under sintering conditions.

Table 4. Mechanical properties of the materials of the first group

Sample	*Sintering* σ^b *(RT) temperature*		K_{1C} $(MPa\,m^{1/2})$	H_V10 *(GPa)*
	(°C)	*(MPa)*		
Gas-pressure sintering				
Si_3N_4	1800	644±138	6·8±0·1	
	1850	736±45	7·7±0·3	14·0±0·7
	1900	836±33	7·9±0·0	
C/N-30/70	1800	644±98	7·0±0·1	
	1850	760±58	7·9±0·4	14·7±0·9
	1900	715±35	8·3±0·1	
C/N-50/50	1800	569±43	6·2±0·4	
	1850	544±29	7·0±0·5	11·4±0·8
	1900	670±51	7·8±0·7	
Hot-pressing				
Si_3N_4		980±65	7·8±0·7	14·6±0·4
T20/C		873±46	6·7±0·3	15·2±0·6
T30/C		763±68	7·3±0·5	14·6±0·6
T40/C		758±53	7·2±0·5	14·9±0·2

Acknowledgement

The authors thank the AIF for supporting the work (Contract Number 54D).

References

1. Ziegler, G., Entwicklungstendenzen der Hochleistungskeramik. *cfi/Ber. DKG*, **68**(3) (1991) 72–9.
2. Petzow, G., Neue Werkstoffe durch Gefügedesign—Chancen und Grenzen. *Ber. Bunsenges. Phys. Chem.*, **93** (1989) 1173–81.
3. Wötting, G., Kanka, B. & Ziegler, G., Microstructural development, microstructural characterisation and relation to mechanical properties of dense Si_3N_4. In *Proceedings of the Int. Conf. Non-Oxide Technical and Engineering Ceramics*, ed. S. Hampshire. Elsevier, London–New York, 1986, pp. 83–6.
4. Wötting, G. & Ziegler, G., Einfluß der Ausgangszusammensetzung und der Herstellungsbedingungen auf die Gefügeausbildung und die mechanischen Eigenschaften von dichtem Siliziumnitrid. *Forschungsberichte der DKG*, **1** (1985) 33–42.
5. Jaroschenko, V., Gogotsi, Y. & Osipova, I., Effect of TiN addition on the properties of silicon nitride-based ceramics. *Mat. Sci. Monographs*, **66C** (1991) 1631–40.
6. Bellosi, A., Guicciardi, S. & Tampieri, A., Development and characterization of electroconductive Si_3N_4–TiN-composites. *J. Eur. Ceram. Soc.*, **9** (1992) 83–93.
7. Gogotsi, Y. G., Grigorjew, O. N. & Jaroschenko, V. P., Particulate ceramic matrix composites. In *Proc. Int. Conf. Euromat 91*, Cambridge, July 1991, pp. 207–9.
8. Saruhan, B. & Ziegler, G., Processing of silicon nitride matrix composites with various reinforcing components. Poster presented at the DLR-Werkstoff-Kolloquium, Cologne, December 1990.
9. McMurty, C. H., Boecker, W. D. G., Seshadri, S. G., Zanghi, J. S. & Garnier, J. E., Microstructure and material properties of SiC–TiB_2 particulate composites. *Am. Ceram. Soc. Bull.*, **66**(2) (1987) 325–9.
10. Schubert, Chr., Pabst, J., Hermel, W. & Klein, U., Computergestützte Bewertung des Verdichtungsprozesses beim Heißpressen von Siliziumnitrid. *cfi/Ber. DKG*, **66**(10) (1989) 420–4.
11. Barin, I. & Knacke, O., *Thermochemical Properties of Inorganic Substances*. Springer Verlag, Berlin–Heidelberg–New York, 1973.
12. Balzer, B., MSc thesis, TU Dresden, FhE/IKTS Dresden, 1992.
13. Herrmann, M., Schubert, Chr., Pabst, J., Richter, H. J., Obenaus, P. & Jaroschenko, V. P., Gefügeverstärkte Kompositkeramic auf der Basis von Si_3N_4. In *Symposium Verstärkung Keramischer Werkstoffe*, Hamburg, October 1991, Tagungsband, DGM-Informationsgesellschaft Verlag, pp. 235–48.
14. Seifert, H. J., Hoffmann, M. J., Lukas, H. L. & Petzow, G., Phase Equilibria in the System Si–Ti–C–N. *Eur. Ceram. Soc., Second Conf.*, 1991.
15. Jean, J. H. & Gupta, T. K., Liquid-phase sintering in the glass-cordierite system: particle size effect. *J. Mat. Sci.*, **27** (1992) 4967–73.
16. Tuan, W. H. & Brook, R. J., Sintering of heterogeneous ceramic compact. *J. Mat. Sci.*, **24** (1989) 1953–8.